communications biology

A Nature Portfolio journal

Article

https://doi.org/10.1038/s42003-025-08806-1

# Social memory engram formation impairment in neuroligin-3 R451C knock-in mice is caused by disrupted prefrontal NMDA receptor-dependent potentiation



Zhiyuan Li[1,4], Qun Yang[1,4], Huiyi Li[1,4], Jiali Ge[1], Hangtian Yan[1], Jiahui Li[2], Yuzhen Fu[1], Kexian Yan[1], Sien Li[1], Jialin Chen[1], Wenjie Dou[1], Junyu Xu[3], Jianhong Luo[2], Baoming Li[1] ✉ & Wei Cao[1] ✉

Autism spectrum disorders (ASDs) are characterized by profound social cognitive deficits, including impairments in social memory—the ability to recognize and remember familiar conspecifics. However, the mechanisms underlying these deficits remain poorly understood. Here, we identify a distinct population of medial prefrontal cortical neurons that encode individual conspecifics and form social memory engram cells (SMECs) through N-methyl-D-aspartate receptor (NMDAR)-dependent long-term potentiation (LTP). Using the Neuroligin 3 R451C knock-in mouse model of autism, we demonstrate that disrupted NMDAR-dependent LTP impairs the formation of SMECs, leading to social memory deficits. Notably, these deficits are rescued by a well-tolerated, once-weekly "pulsed" administration of D-cycloserine, a partial NMDAR agonist. Our findings underscore the pivotal role of NMDAR-dependent synaptic plasticity in social memory encoding and position NMDAR-targeted therapies as a compelling avenue for addressing social cognitive deficits in ASDs.

Autism spectrum disorders (ASDs) represent a complex neurodevelopmental condition with enduring, lifelong impacts. The prevalence of ASDs continues to rise annually, accompanied by substantial heterogeneity[1]. Social memory—the ability to recognize and remember familiar conspecifics—is essential for maintaining stable and dynamic social networks[2,3] and is a fundamental aspect of social cognition that is impaired in ASDs[4–6]. However, the precise mechanisms underlying social memory deficits in ASDs remain largely unexplored, underscoring the pressing need for research to elucidate these mechanisms and inform the development of targeted therapeutic interventions.

The medial prefrontal cortex (mPFC), recognized as the brain's executive center, plays a critical role in social novelty behaviors[7–11]. The ability to distinguish between familiar and unfamiliar conspecifics, form social memories, and exhibit a preference for novel conspecifics underpins social novelty behavior in mice. Studies have indicated that a subpopulation of prefrontal cortical neurons is essential for social memory, and manipulation of these neurons can regulate social memory in mice[12]. The release of corticotropin-releasing hormone from the mPFC to the lateral septum suppresses social interaction with familiar, but not novel, mice, thereby supporting social novelty preference[13]. Yet, it remains unclear whether mPFC neurons satisfy the criteria of social memory engrams and are directly involved in encoding individual social memories. Recent advancements in memory engram technology allow for the discrete and genetic targeting of subsets of activity-dependent neuronal ensembles[14]. Accumulating evidence suggests that prefrontal engram cells are generated at the onset of learning, gradually maturing over time as they undergo enduring physical and chemical changes, ultimately becoming indispensable for memory expression[15–18]. These discoveries offer a foundation for exploring the neural mechanisms, both at cellular and synaptic levels, that facilitate the long-term storage and retrieval of social memories within the mPFC.

Neuroplasticity, particularly N-methyl-D-aspartate receptor (NMDAR)-dependent long-term potentiation (LTP), plays a pivotal role in learning and memory[19–21]. NMDAR function is closely associated with the social deficits observed in ASDs, and genetic variations linked to ASDs are located in genes encoding NMDAR subunits[22–25]. Additionally, research has shown that NMDAR-dependent synaptic potentiation is necessary for the

[1]Institute of Brain Science and Department of Physiology, School of Basic Medical Sciences, Hangzhou Normal University, Hangzhou, China. [2]Laboratory of Translational Psychiatry, Affiliated Mental Health Center & Hangzhou Seventh People's, School of Brain Science and Brain Medicine, Zhejiang University School of Medicine, Hangzhou, China. [3]Pillar of STEM Education, College of Education Sciences, Hong Kong University of Science and Technology (Guangzhou), Guangzhou, China. [4]These authors contributed equally: Zhiyuan Li, Qun Yang, Huiyi Li. ✉e-mail: bmli@hznu.edu.cn; caowei@hznu.edu.cn

accessibility of a prefrontal neuronal assembly in retrieving fear extinction[17], indicating that engram cells undergo specific synaptic functional changes. Our previous study reported that NMDAR hypofunction in the mPFC constitute a central node in the pathogenesis of social novelty deficits in the Neuroligin 3 (NL3) R451C knock-in (KI) mouse model of autism[8,9]. However, the underlying mechanisms by which NMDAR dysfunction contributes to impairments in social memory, particularly whether through the regulation of social engram cells, remain poorly understood.

We identified a neuronal population in the mPFC that encodes individual conspecifics through NMDAR-dependent synaptic potentiation, forming reservoirs for long-term social memory. In KI mice, deficits in social memory stemmed from impaired NMDAR-dependent LTP, disrupting the formation of social memory engram cells (SMECs). These impairments were reversed by a well-tolerated, once-weekly "pulsed" administration of the NMDAR agonist D-cycloserine. Our findings underscore the essential role of NMDAR-dependent LTP in prefrontal SMEC formation and highlight NMDAR-targeted therapies as a promising avenue for addressing social memory deficits in ASDs.

## Results

### Chemogenetic reactivation of mPFC social exploration-associated neurons enables social memory retrieval

To investigate whether individual information is encoded in a distinct population of sparse neurons in the mPFC, we employed engram technology to explore the single-cell mechanisms underlying social memory. In order to selectively label neurons associated with social exploration in the mPFC for subsequent analysis, we utilized an adeno-associated virus (AAV)-based RAM system. This system integrates a synthetic promoter, activated by neuronal activity, with a downstream reporter gene regulated by a doxycycline (Dox)-dependent Tet-off system[17,26,27]. Wild-type (WT) mice were bilaterally injected with AAV-RAM-GFP into the mPFC and maintained on Dox-containing drinking solution for 48 h before and after viral injection. The mice were then switched to Dox-free drinking solution 24 h prior to and following a 10 min social interaction on Day 1, after which they returned to Dox drinking until the subsequent social interaction, either with the same familiar mouse or a novel mouse, for 10 min on Day 7. Brain tissues were collected and fixed 90 min following the social interaction for c-Fos immunostaining on Day 7 (Fig. 1A).

Our analysis revealed that, compared to controls with no social exposure, social investigation in both groups resulted in robust labeling of neurons within the deep layers of the mPFC, with no significant difference between groups (Fig. 1B, Supplementary Fig. 1A), suggesting that these labeled cells are selectively responsive to neuronal activity elicited by social stimuli. We observed that the labeled cells predominantly accumulated in the prelimbic region (Supplementary Fig. 1B). The identity of these captured neurons was further confirmed through immunohistochemistry, revealing that approximately 60% of the $GFP^+$ neurons expressed CamKII, while 40% expressed GAD67 (Supplementary Fig. 1C). These results collectively underscore the predominance of excitatory neurons within the social-labeled population. Moreover, mice re-exposed to the same familiar conspecific exhibited an increase in overall c-Fos activation compared to those exposed to a novel mouse (Supplementary Fig. 1D). Notably, the proportion of reactivated neurons—defined by overlapping GFP and c-Fos signals—was significantly greater in mice encountering the familiar individual, suggesting the presence of "engram cells" within the mPFC that are selectively re-engaged by repeated social experience (Fig. 1C).

To determine whether the putative engram cells are functionally sufficient for the retrieval of social memory, we employed a dual-viral strategy, co-injecting AAV-RAM-Cre-GFP and AAV-DIO-hM3Dq-mCherry into the mPFC of WT mice. After a one-week interval following the initial social interaction, during which the stimulus mice were removed, hM3Dq-expressing mice were administered either saline or deschloroclozapine (DCZ), a potent and selective chemogenetic actuator, 1.5 h prior to performing social memory tasks (Fig. 1D, E). These results suggest that social memory cannot be retrieved by natural cues after one week in the saline-treated group. In contrast, mice with artificially reactivated labeled cells successfully retrieved social memory, as evidenced by their preference for the novel mouse and a heightened discrimination index during the three-chamber test (Fig. 1F, G). Taken together, these findings provide compelling evidence that individual information is encoded in a distinct population of sparse neurons within the mPFC, and that the reactivation of these cells is sufficient to reinstate the retrieval of social memory.

### Chemogenetic inhibition of mPFC social exploration-associated neurons impairs social memory retrieval

To further investigate the underlying mechanisms of social memory, we refined the social behavioral paradigm, enabling mice to form long-lasting social memories. Using an AAV-based RAM system, we selectively labeled neurons engaged in social interactions. WT mice were exposed to the same conspecific for 10 min daily over a five-day period, with the social neurons labeled on Day 5. After a one-week interval, the mice were reintroduced to either the same familiar mouse or a novel conspecific for 10 min on Day 12. Brain tissues were harvested and fixed 90 min following the social interaction for subsequent c-Fos immunostaining (Fig. 2A). As the frequency of social interactions increased, the WT mice grew progressively more familiar with the caged unfamiliar conspecific, leading to a significant reduction in sniffing time. On Day 12, mice exposed to the familiar conspecific continued to show relatively low sniffing time, whereas those encountering a novel mouse exhibited a substantial increase in sniffing duration compared to the former group (Fig. 2B). These findings suggest that this protocol effectively induces long-lasting social memory in mice, which remains stable for at least 7 days.

Consistent with our previous observations, analysis revealed that, compared to controls with no social exposure during the labeling period, social investigation in both groups led to distinct neuronal labeling within the mPFC, with no significant difference between groups (Fig. 2C, Supplementary Fig. 2A). This suggests that the labeled cells are selectively responsive to neuronal activity induced by social stimuli. Importantly, although the number of c-FOS-positive cells remained unaltered (Supplementary Fig. 2B), the proportion of reactivated neurons—defined by the co-localization of GFP and c-Fos signals—was significantly elevated in mice exposed to the same familiar conspecific, relative to those encountering a novel conspecific (Fig. 2D). These findings provide compelling evidence for the existence of "engram cells" within the mPFC, which can be reactivated by the same social stimuli.

To evaluate whether the putative engram cells are essential for the retrieval of social memory, we utilized a dual-viral approach, co-delivering AAV-RAM-Cre-GFP and AAV-DIO-hM4Di-mCherry into the mPFC of WT mice. Mice were individually housed and exposed to the same unfamiliar conspecific each day over five consecutive days. After a one-week interval, during which the stimulus mice were removed, hM4Di-expressing mice received either saline or DCZ 1.5 h prior to engaging in the social memory tasks (Fig. 2E, F). These findings indicate that in the saline-treated group, social memory can be reinstated by natural cues after a one-week delay. Conversely, when the engram cells were artificially inhibited, mice exhibited an inability to retrieve social memory, as evidenced by their lack of preference for the novel conspecific and a marked reduction in the discrimination index during the three-chamber test (Fig. 2G, H). Taken together, these results strongly support the notion that individual conspecific information is encoded in a specific population of sparse neurons within the mPFC, and that the reactivation of these cells is crucial for the retrieval of social memory.

### Synaptic strength is increased in prefrontal social engram cells

To investigate the differential neural activity between putative social memory engram cells (SMECs) and non-SMECs, we combined the RAM system with electrophysiological recordings (Fig. 3A, B). Our analysis revealed that SMECs exhibited markedly elevated input/output curves of evoked a-amino-3-hydroxy-5-methyl-4-isoxazolepropionic acid (AMPA)-receptor-mediated synaptic responses, in contrast to their neighboring non-

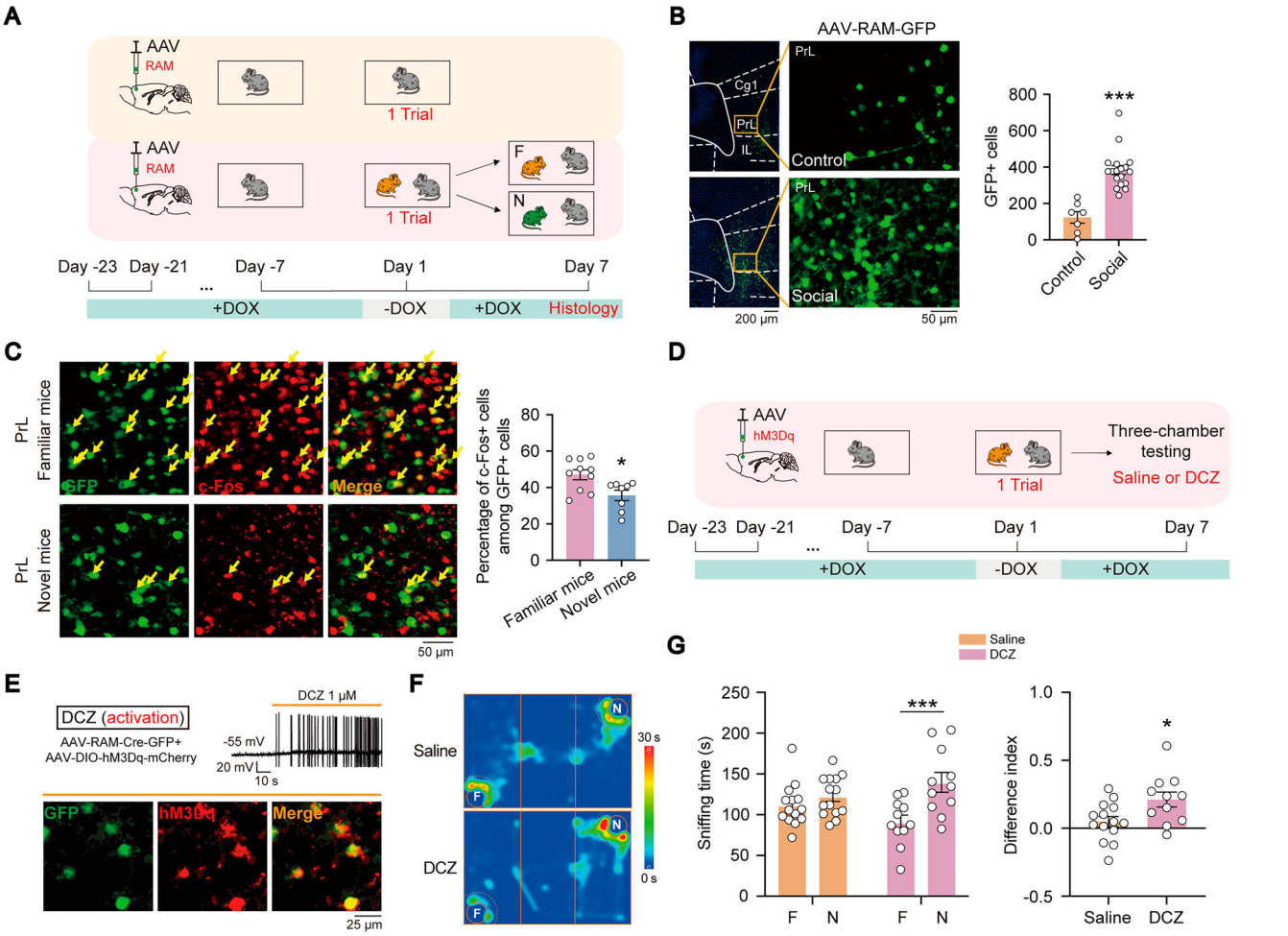


**Fig. 1 | Reactivating mPFC social exploration-associated neurons enables social memory retrieval. A** Experimental design for social-associated ensemble labeling. Doxycycline was taken off 24 h before the social test on Day 1 and placed back 24 h after it. **B** Left: Images of neurons in the mPFC activated during the social and control tests on Day 1. DAPI (blue) was used to label nuclei (scale bars, 50 and 200 μm). Cg1, cingulate cortex, area 1; PrL, prelimbic cortex; IL, infralimbic cortex. Right: The number of GFP-positive cells was significantly increased in the social group (Two-tailed Mann-Whitney test,$p < 0.0001$). **C** Left: Representative images of the prelimbic cortex (PrL) following dual exposure to social stimuli from the familiar mice (top) and novel mice (bottom). The cells activated by social stimuli on Day 1 were marked with GFP (green), while the c-Fos expression induced by social stimuli on Day 7 was revealed through immunostaining (red). Yellow arrows indicate cells co-labeled with GFP and c-Fos ($GFP^+$ $Fos^+$) (scale bar, 50 μm). Right: A greater number of neurons were reactivated ($GFP^+$ $Fos^+$) during social stimuli exposure from the familiar mice compared to those from novel mice (Two-tailed unpaired *t* test, $t = 2.853$, df = 16, $p = 0.012$). **D** Experimental design for activating social-associated ensemble. Doxycycline was taken off 24 h before the social test on Day 1 and placed back 24 h after it. Saline or DCZ was administered via intraperitoneal injection 90 min prior to the social behavior assessment on Day 7. **E** Top: Sample trace shows validation of virus by electrophysiological recording. Bottom: Representative images of neurons in the mPFC co-expressing hM3Dq and GFP (scale bar, 25 μm). **F** Representative heatmaps of three-chamber tests performed in saline- and DCZ-treated mice. **G** Sniffing time (left) and difference index (right) after chemogenetic reactivation of mPFC social exploration-associated neurons in three-chamber tests (Left: two-way ANOVA, Interaction: $F_{(1, 46)} = 4.911$, $p = 0.032$; Drug: $F_{(1, 46)} = 0.050$, $p = 0.824$; Familiar vs. Novel: $F_{(1, 46)} = 12.41$, $p = 0.001$; Right: Two-tailed unpaired *t* test, $t = 2.504$, df = 23, $p = 0.020$). ± SEM. $^*p < 0.05$, $^{***}p < 0.001$. *n* = number of mice.

SMECs (Fig. 3C). These findings suggest that putative SMECs possess enhanced synaptic efficacy. Additionally, the paired-pulse ratio analysis showed no significant differences between the two groups (Fig. 3D). Furthermore, we successfully induced LTP in non-SMECs, an effect that was entirely blocked by pretreatment with the NMDAR antagonist, AP-5 (Fig. 3E), confirming the NMDAR dependence of this LTP. In contrast, LTP induction was absent in SMECs (Fig. 3E), a phenomenon indicative of LTP occlusion. This phenomenon of LTP occlusion has been interpreted as evidence that prior learning-induced LTP imposes a ceiling on the capacity for subsequent LTP induction within these cells[17,28,29]. Collectively, these results suggest that repeated social stimuli evoke LTP in mPFC neurons associated with social exploration, triggering enduring physical and chemical alterations essential for the encoding of social memories related to specific conspecifics—an effect that aligns with the defining characteristics of social engram cells.

## Social memory is impaired in NL3 R451C KI mouse model of autism

We selected the classic autism model, the NL3 R451C KI mice, to explore the specific mechanisms underlying social memory deficits in ASDs. We investigated the deviations in social behavior exhibited by the NL3 R451C KI mice. Consistent with our previous studies[8,9], the KI mice displayed normal sociability but exhibited pronounced deficits in social novelty preference during the three-chamber test (Fig. 4A). Furthermore, we employed the previously described long-term social memory paradigm to more comprehensively assess social memory. A subject mouse was introduced to a novel conspecific (Stranger 1, S1) for a duration of 10 min. Over five consecutive days, the experimental mouse was repeatedly exposed to the same conspecific (S1), allowing it to habituate to both the environment and the social stimulus. One week later, the subject mouse was reintroduced to S1 to evaluate long-term social memory. While WT mice showed diminished

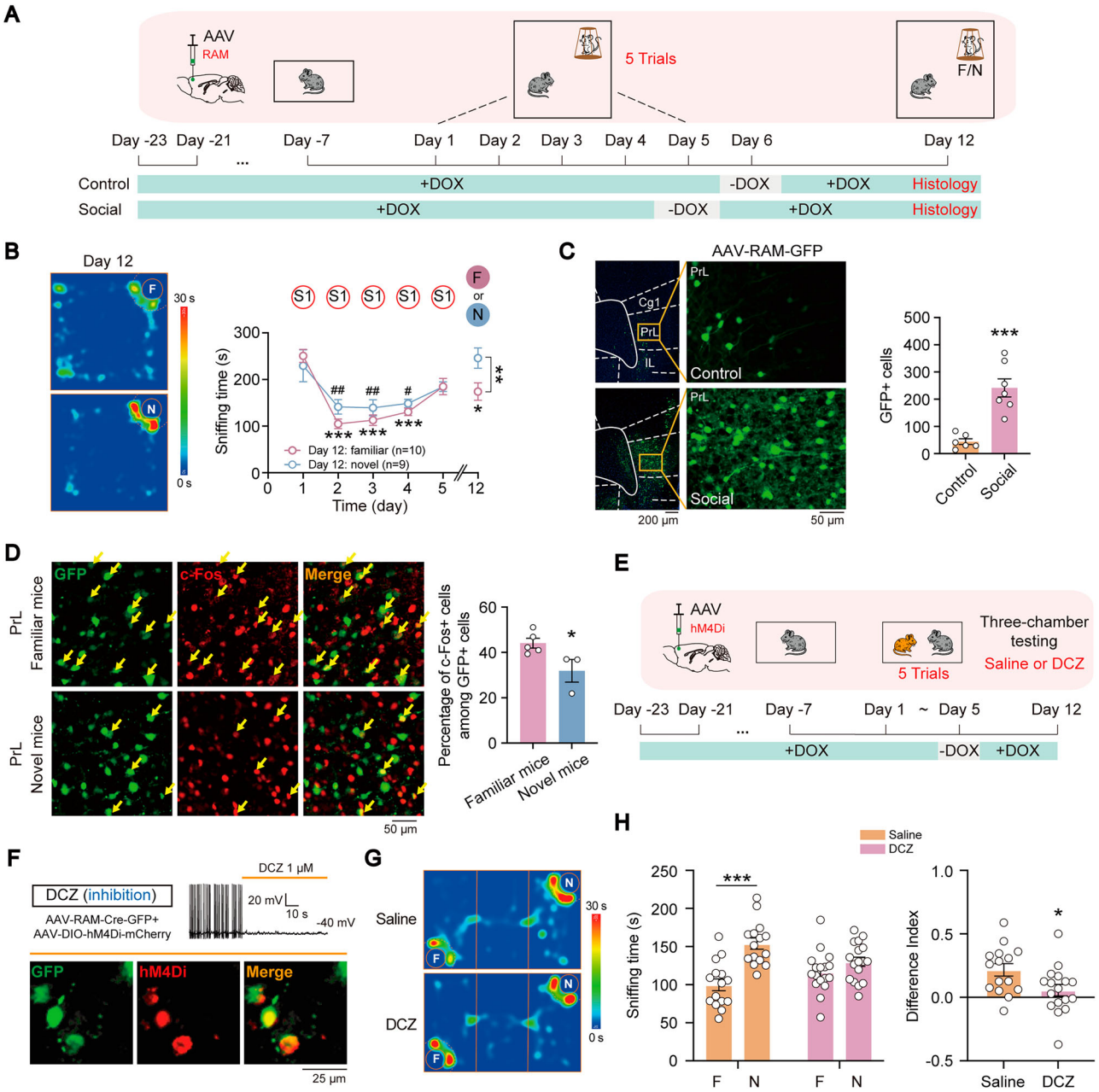


**Fig. 2 | Inactivation of mPFC social exploration-associated neurons impairs social memory retrieval. A** Experimental design for social-associated ensemble labeling. Doxycycline was taken off 24 hours before the social test on Day 5 or the control test on Day 6 and placed back 24 h after it. **B** Left: Representative heatmaps from the long-term social memory tests conducted on Day 12, depicting interactions with familiar and novel mice, respectively. Right: Sniffing time in the open-field arena (two-way ANOVA, Interaction: $F_{(5,\ 102)} = 1.785$, $p = 0.123$; Time (day): $F_{(5,\ 102)} = 16.43$, $p < 0.0001$; Group 1 vs. Group 2: $F_{(1,\ 102)} = 5.015$, $p = 0.027$). Specifically, * indicates significance within Group 1 (familiar), and # indicates significance within Group 2 (novel), both relative to the Day 1 baseline. An asterisk (*) also denotes significance between groups. **C** Left: Images of neurons in the mPFC activated during the social test on Day 5 and the control test on Day 6. DAPI (blue) was used to label nuclei (scale bars, 50 and 200 μm). Right: The number of GFP-positive cells was significantly increased in the social group (Two-tailed Welch's t test, t = 5.680, df = 7.224, $p = 0.0007$). **D** Left: Representative images of the prelimbic cortex (PrL) following dual exposure to social stimuli from the familiar mice (top) and novel mice (bottom). The cells activated by social stimuli on Day 5 were marked with GFP (green), while the c-Fos expression induced by social stimuli on Day 12 was revealed through immunostaining (red). Yellow arrows indicate cells co-labeled with GFP and c-Fos ($GFP^+$ $Fos^+$) (scale bar, 50 μm). Right: A greater number of neurons were reactivated ($GFP^+$ $Fos^+$) during social stimuli exposure from the familiar mice compared to those from novel mice (Two-tailed Mann-Whitney test, $p = 0.036$). **E** Experimental design for inhibiting social-associated ensemble. Saline or DCZ was administered prior to the social behavior assessment. **F** Top: Sample trace shows validation of virus by electrophysiological recording. Bottom: Representative images of neurons in the mPFC co-expressing hM4Di and GFP (scale bar, 25 μm). **G** Representative heatmaps of three-chamber tests performed in saline- and DCZ-treated mice. **H** Sniffing time (left) and difference index (right) after chemogenetic inhibition of mPFC social exploration-associated neurons in three-chamber tests (Left: two-way ANOVA, Interaction: $F_{(1,\ 60)} = 8.497$, $p = 0.005$; Drug: $F_{(1,\ 60)} = 0.259$, $p = 0.613$; Familiar vs. Novel: $F_{(1,\ 60)} = 23.56$, $p < 0.0001$; Right: Two-tailed unpaired t test, t = 2.425, df = 30, $p = 0.022$).All data were mean ± SEM. $^{*/\#}p < 0.05$, $^{**/\#\#}p < 0.01$, $^{***}p < 0.001$. *n* = number of mice.

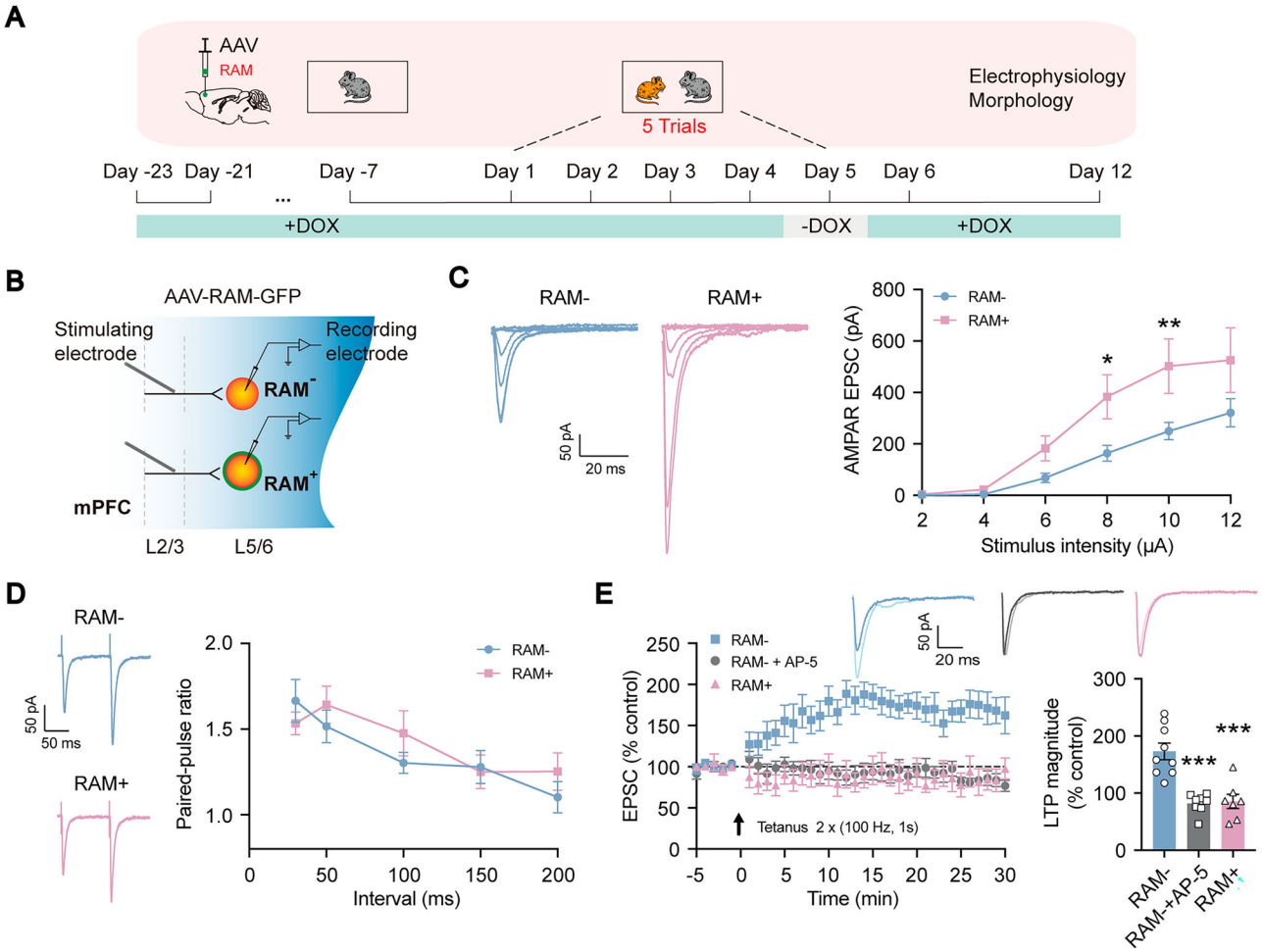


**Fig. 3 | Synaptic strength is enhanced in prefrontal social engram cells.** **A** Experimental design for social-associated ensemble labeling. Doxycycline was taken off 24 hours before the social test on Day 5 and placed back 24 h after it. **B** Electrophysiological experimental design for recording labeled neurons in layers V/VI and adjacent unlabeled neurons of the mPFC on Day 12, with a concentric bipolar electrode positioned in layers II/III. **C** Representative traces (left) and statistical graph (right) of Input-output curves of evoked AMPA-receptor-mediated synaptic responses recorded from RAM$^+$ and nearby RAM$^-$ pyramidal neurons in the mPFC (two-way ANOVA, Interaction: $F_{(5,\ 122)} = 2.064$, $p = 0.074$; Stimulus intensity: $F_{(5,\ 122)} = 22.68$, $p < 0.0001$; RAM$^-$ vs. RAM$^+$: $F_{(1,\ 122)} = 19.38$, $p < 0.0001$; $n = 13$ and 11 neurons recorded from 4 mice). **D** Representative traces (left) and statistical graph (right) of PPR recorded from RAM$^+$ and nearby RAM$^-$ pyramidal neurons in the mPFC (two-way ANOVA, Interaction: $F_{(4,\ 89)} = 0.824$,$p = 0.513$; Interval: $F_{(4,\ 89)} = 6.596$, $p = 0.0001$; RAM$^-$ vs. RAM$^+$: $F_{(1,\ 89)} = 0.786$, $p = 0.378$; $n = 11$ and 9 neurons recorded from 4 mice). **E** High-frequency stimulation fails to induce NMDAR-dependent LTP in the RAM$^+$ pyramidal neurons in the mPFC. Top: Representative traces of averaged EPSCs recorded 5 minutes before (dark traces) and 25 min after (light traces) LTP induction. Below: Changes in EPSC amplitude induced by 100 Hz stimulation and quantification of EPSCs 25 min after stimulation compared to the respective values before stimulation in RAM$^-$, RAM$^-$ +AP5 and RAM$^+$ pyramidal neurons (one-way ANOVA, Between columns: $F_{(2,\ 21)} = 19.96$, $p < 0.0001$; RAM$^-$ vs. RAM$^-$ +AP5: $p < 0.0001$; RAM$^-$ vs. RAM$^+$: $p = 0.0001$; n, number of neurons recorded from 6 mice per group).All data were mean ± SEM. $^*p < 0.05$, $^{**}p < 0.01$, $^{***}p < 0.001$.

interest in S1 due to increased familiarity, they retained curiosity towards the newly introduced conspecific, S2 (Fig. 4B). In contrast, the KI mice demonstrated significantly prolonged interactions with S1 on Days 4, 5, and 11, indicative of impaired social memory, despite exhibiting normal sociability. Both WT and KI mice spent comparable amounts of time with S1 on Day 1 and with S2 on Day 12 (Fig. 4B), underscoring the memory-specific deficit in the KI mice.

### Impaired NMDAR-dependent LTP disrupts the formation of social engram cells in the mPFC of NL3 R451C KI mice

To investigate the specific mechanisms underlying the social memory deficit in the KI mice, we first employed an AAV-based RAM system to selectively label neurons engaged in social interactions (Fig. 5A). In contrast to WT mice, there was no significant difference in the number of social-labeled cells in the mPFC of the KI mice (Fig. 5B). Furthermore, the proportion of reactivated neurons exhibiting co-expression of GFP and c-Fos signals in response to exposure to a familiar conspecific was similar in both KI and WT mice (Fig. 5C). These findings indicate that there is no aberration in the number of cells engaged during social interactions in the mPFC of KI mice, which aligns with the absence of changes in social motivation, and suggests that the information regarding specific social partners is encoded within these putative engram cells.

So, which specific process is disrupted, leading to the social memory deficit in the KI mice? We have previously reported that NMDAR hypofunction occurs in both pyramidal neurons and PV-positive interneurons within the mPFC of NL3 R451C KI mouse model of autism[8]. We next sought to determine whether NMDAR-dependent synaptic plasticity is altered in these KI mice, as we have previously suggested that the formation of social memory engram cells requires LTP. Using in vitro whole-cell patch-clamp recordings, we applied a LTP induction protocol to evoke synaptic plasticity in pyramidal neurons (Fig. 5D). Our results revealed a significant impairment of LTP induced by high-frequency stimulation in the KI mice (Fig. 5E). To assess the potential for rescue, we treated acute mPFC brain slices from the KI mice with D-cycloserine, a partial agonist at the

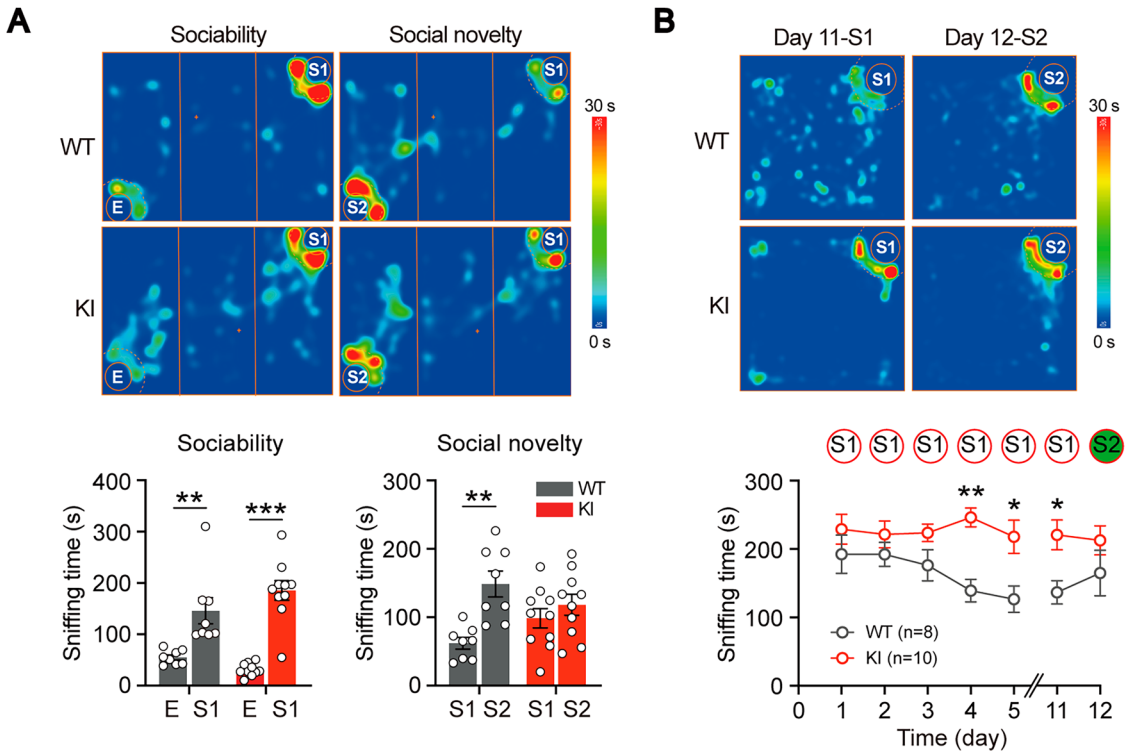


**Fig. 4 | Social memory is impaired in NL3 R451C KI mouse model of autism.** **A** Top: Representative heatmaps of the three-chamber tests performed in the WT/KI mice. Bottom: The KI mice exhibited social novelty deficits, as analyzed by the three-chamber sociability (Left) and social novelty (Right) tests (Left: two-way ANOVA, Interaction: $F_{(1, 32)} = 3.982$, $p = 0.055$; WT vs. KI: $F_{(1, 32)} = 0.247$, $p = 0.623$; Empty vs. Stranger 1: $F_{(1, 32)} = 59.66$, $p < 0.0001$; Right: two-way ANOVA, Interaction: $F_{(1, 32)} = 5.053$, $p = 0.032$; WT vs. KI: $F_{(1, 32)} = 0.045$, $p = 0.834$; Stranger 1 vs. Stranger 2: $F_{(1, 32)} = 12.71$, $p = 0.001$). **B** Top: Representative heatmaps of the long-term social memory tests performed in the WT/KI mice. Bottom: The KI mice exhibited impaired long-term social memory (two-way ANOVA, Interaction: $F_{(6, 112)} = 1.015$, $p = 0.420$; Time (day): $F_{(6, 112)} = 0.890$, $p = 0.505$; WT vs. KI: $F_{(1, 112)} = 31.03$, $p < 0.0001$).All data were mean ± SEM. $^{*}p < 0.05$, $^{**}p < 0.01$, $^{***}p < 0.001$. $n$ = number of mice.

glycine-binding site of NMDARs. Remarkably, 20 μM DCS effectively restored both NMDAR function[8] and LTP in the mPFC of the KI mice (Fig. 5E). Collectively, these results demonstrate that NMDAR-dependent LTP of pyramidal neurons is profoundly impaired in the mPFC of the KI mice. In addition, we also recorded theta-burst stimulation (TBS)-induced LTP and low-frequency (1 Hz)-induced long-term depression (LTD) in mPFC pyramidal neurons, finding that both forms of plasticity were impaired in KI mice compared to WT controls (Supplementary Fig. 3), suggesting a convergent vulnerability in synaptic plasticity across different induction paradigms.

Further investigation through whole-cell patch-clamp recordings on PV-positive interneurons revealed that the magnitude of LTP induced by high-frequency stimulation in these cells was significantly greater than in pyramidal neurons, reaching approximately 223% (Fig. 5F). Notably, LTP in $PV^{+}$ interneurons was markedly suppressed in the KI mice, although there was a clear trend towards enhancement—albeit not statistically significant—upon treatment with a higher concentration of 60 μM DCS (Fig. 5F). These data strongly suggest a profound blockade of neuroplasticity within the mPFC of the KI mice. Moreover, prior classification of the labeled neuronal populations revealed that the majority of these cells were pyramidal neurons. Accordingly, we focused our subsequent experiments on further elucidating the neuroplasticity within pyramidal neurons.

Collectively, these findings suggest that while the KI mice exhibit no deficits in social motivation, and the number of cells activated in the mPFC in response to specific social partners remains intact, these cells fail to mature into authentic social engram cells due to impaired NMDAR-dependent LTP. This disruption ultimately prevents the formation of social memory in these mice.

## D-cycloserine is optimal for "pulsed" once-weekly administration

To determine the most effective dosing regimen for addressing social memory deficits in autism, we first sought to investigate whether the therapeutic effect of DCS could be sustained over several days, despite its rapid metabolic clearance. We conducted an experiment to assess the enduring impact of a single intraperitoneal injection of 20 mg/kg DCS on mPFC deficits in the KI mice after a span of three days (Fig. 6A). Notably, this treatment successfully restored the NMDA/AMPA ratio in pyramidal neurons within the mPFC of the KI mice (Fig. 6B, C). Furthermore, we observed that the NMDAR-dependent LTP in pyramidal neurons was also rescued by a single DCS injection, three days post-administration (Fig. 6D). These findings underscore the lasting restorative effects of a single dose of D-cycloserine.

Given the potential for agonist-induced desensitization of the glycine-binding site with daily DCS administration[30,31], we sought to explore whether "pulsed" dosing would mitigate such concerns. Given the prolonged restorative effects of DCS on mPFC deficits in the KI mice, we next investigated its impact on social behavior deficits, with particular focus on the duration of its efficacy following a single acute intraperitoneal injection. This has profound implications for clinical therapeutic strategies. To this end, we performed three-chamber social preference tests and measured the NMDA/AMPA ratio as well as LTP in pyramidal neurons at one and three weeks following a single intraperitoneal DCS injection in young adult mice (Fig. 6E). In saline-treated controls, the KI mice exhibited significant deficits in social novelty preference. However, DCS administration effectively ameliorated these deficits one week after injection (Fig. 6F, G, Supplementary Figs. 4A,B). Interestingly, the therapeutic effects on social behavior were no longer observed three weeks post-injection (Fig. 6H, I, Supplementary Figs. 4C and 4D). Electrophysiological assessments revealed that

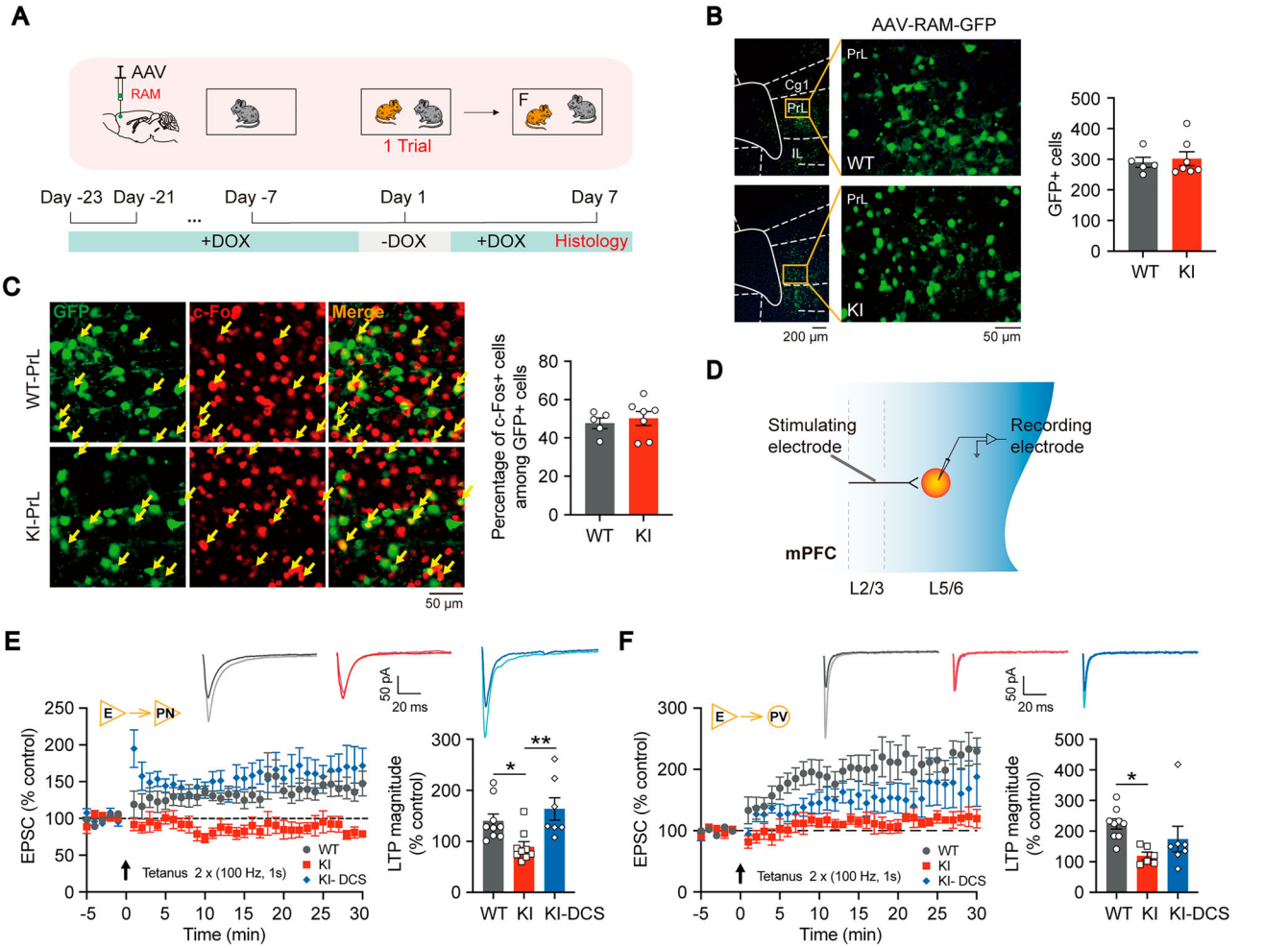


**Fig. 5 | Impaired NMDAR-dependent LTP disrupts the formation of social engram cells in the mPFC of NL3 R451C KI mice. A** Experimental design for social-associated ensemble labeling. Doxycycline was taken off 24 hours before the social test on Day 1 and placed back 24 h after it. **B** Left: Images of neurons in the mPFC of the WT/KI mice activated during the social tests on Day 1. DAPI (blue) was used to label nuclei (scale bars, 50 and 200 μm). Cg1, cingulate cortex, area 1; PrL, prelimbic cortex; IL, infralimbic cortex. Right: The number of GFP-positive cells did not change in the KI group (Two-tailed unpaired t test, t = 0.397, df = 10, $p = 0.700$; n, number of mice). **C** Left: Representative images of the prelimbic cortex (PrL) of the WT (top) and KI (bottom) mice following dual exposure to social stimuli from the same mice. The cells activated by social stimuli on Day 1 were marked with GFP (green), while the c-Fos expression induced by social stimuli on Day 7 was revealed through immunostaining (red). Yellow arrows indicate cells co-labeled with GFP and c-Fos ($GFP^+$ $Fos^+$) (scale bar, 50 μm). Right: The number of reactivated ($GFP^+$ $Fos^+$) neurons during social stimuli exposure was not changed in the KI mice compared to the WT mice (Two-tailed unpaired t test, t = 0.506, df = 10, $p = 0.624$; *n*, number of mice). **D** Cartoon diagram of whole-cell recordings in layer V/VI neurons of the mPFC, with a concentric bipolar electrode placed in layer II/III. **E** Top: Sample traces of averaged EPSCs recorded 5 minutes before (dark traces) and 25 min after (light traces) LTP induction. Below: Changes in EPSC amplitude induced by 100 Hz stimulation and quantification of EPSCs 25 min after stimulation compared to the respective values before stimulation in pyramidal neurons of WT mice, KI mice, and KI slices treated with 20 μM D-cycloserine (one-way ANOVA, Between columns: $F_{(2,\ 22)} = 6.486$, $p = 0.006$; WT vs. KI: $p = 0.049$; KI vs. KI-DCS: $p = 0.006$; n in each bar, number of neurons recorded from 5 mice per group). **F** Top: Sample traces of averaged EPSCs recorded 5 min before (dark traces) and 25 min after (light traces) LTP induction. Below: Changes in EPSC amplitude induced by 100 Hz stimulation and quantification of EPSCs 25 min after stimulation compared to the respective values before stimulation in $PV^+$ interneurons of WT mice, KI mice, and KI slices treated with 60 μM D-cycloserine (one-way ANOVA, Between columns: $F_{(2,\ 19)} = 3.750$, $p = 0.042$; WT vs. KI: $p = 0.034$; KI vs. KI-DCS: $p = 0.379$; n in each bar, number of neurons recorded from 5 mice per group).All data were mean ± SEM. $^*p < 0.05$, $^{**}p < 0.01$.

the rescue effect of a single DCS dose on NMDAR hypofunction in the mPFC of the KI mice persisted for at least one week (Fig. 6J), suggesting the involvement of transcriptional and expression mechanisms. However, therapeutic efficacy diminished by the third week (Fig. 6J). Additionally, we found that NMDAR-dependent LTP in pyramidal neurons was similarly restored one-week post-DCS administration but was no longer sustained at three weeks (Fig. 6K), mirroring the pattern observed for NMDAR function.

These results indicate the necessity of evaluating the resistance induced by long-term weekly administration. To address this, both WT and KI mice received a weekly intraperitoneal injection of D-cycloserine (20 mg/kg) or an equivalent volume of saline for three consecutive weeks, followed by behavioral and electrophysiological assessments one-week post-administration (Fig. 7A). We explored the efficacy of "pulsed" once-weekly DCS administration. Remarkably, DCS remained effective in reversing social novelty deficits in KI mice one week after completing three consecutive weekly doses (Fig. 7B, C, Supplementary Fig. 5). Furthermore, the therapeutic effects of DCS on the NMDA/AMPA ratio and NMDAR-dependent LTP in pyramidal neurons were in parallel with its impact on social novelty preference (Fig. 7D, E).

Our findings support that "pulsed" once-weekly administration of DCS represents a viable and well-tolerated regimen. From both a mechanistic and behavioral standpoint, we have demonstrated that this dosing strategy is optimal for mitigating social memory deficits in the KI mouse model.

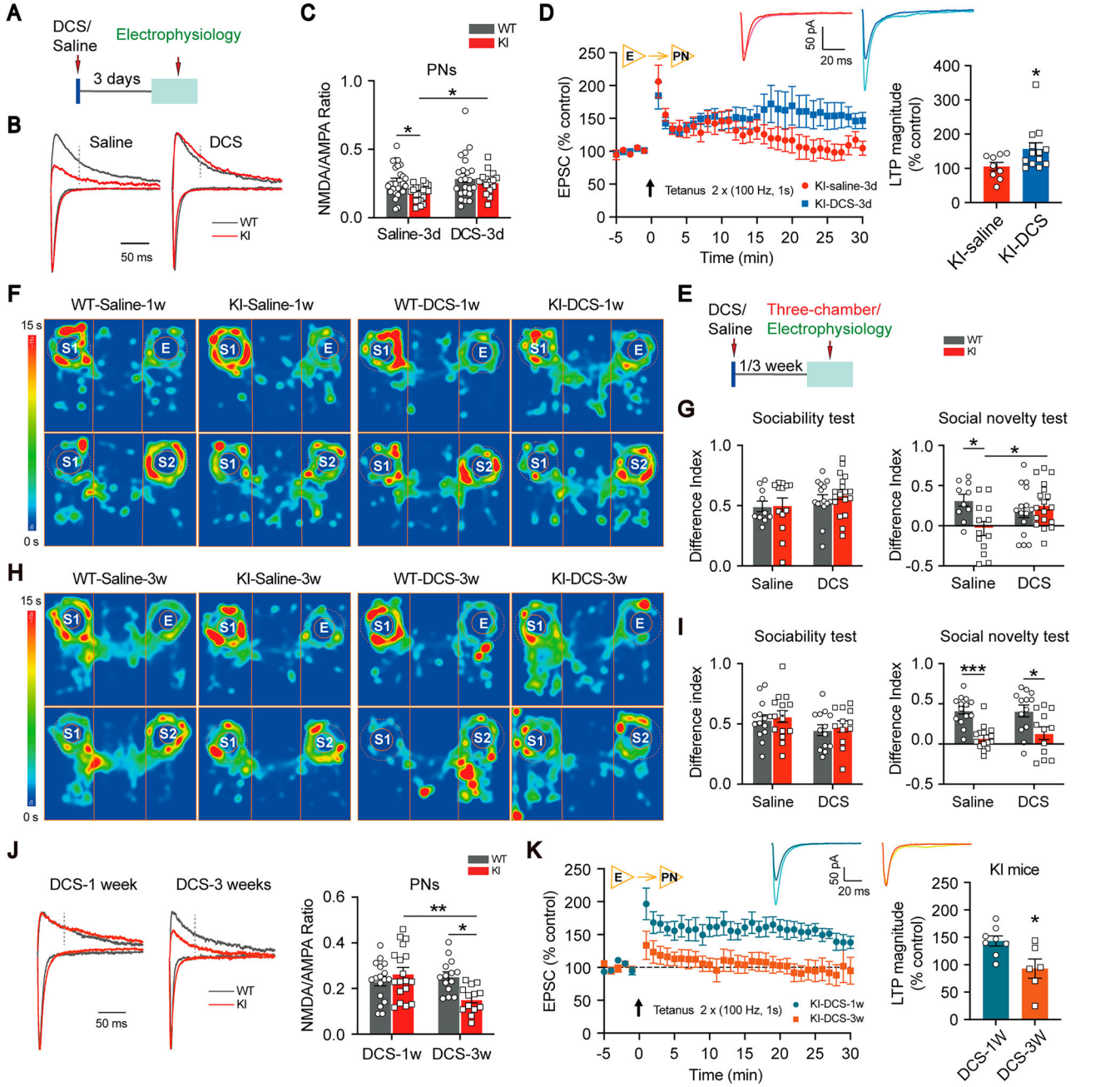


**Fig. 6 | Long-term rescue effects of D-Cycloserine on mPFC deficits and social behaviors in NL3 R451C KI mice. A** The flowchart of electrophysiological tests for examining of rescue effect three days after D-cycloserine administration. Sample traces (**B**) and bar graph (**C**) of measurements of NMDA/AMPA receptor response ratios recorded from pyramidal neurons in the mPFC of P60-P70 mice three days after one-dose saline or D-cycloserine administration (two-way ANOVA, Interaction: $F_{(1, 81)} = 1.228$, $p = 0.271$; Drug: $F_{(1, 81)} = 4.355$, $p = 0.040$; WT vs. KI: $F_{(1, 81)} = 5.658$, $p = 0.020$; *n*, number of neurons recorded from 4 saline-treated littermates and 4 DCS-treated littermates, respectively). **D** Top: Sample traces of averaged EPSCs recorded 5 min before (dark traces) and 25 min after (light traces) LTP induction. Below: Changes in EPSC amplitude induced by 100 Hz stimulation and quantification of EPSCs 25 min after stimulation compared to the respective values before stimulation in pyramidal neurons of the KI mice three days after one-dose administration of saline or D-cycloserine (Two-tailed unpaired *t* test, t = 2.135, df = 20, $p = 0.045$; *n* in each bar, number of neurons recorded from 4 saline-treated KI mice and 8 DCS-treated KI mice, respectively). **E** The flow chart of three-chamber/electrophysiological tests for examining the rescue effect one week or three weeks after D-cycloserine administration. **F–I** Representative heat-maps (**F** and **H**) and statistical bar charts (**G** and **I**) illustrating the results of the three-chamber social interaction tests conducted in WT/KI mice, one or three weeks following a single administration of Saline/DCS (two-way ANOVA. For one-week data, $p = 0.736$ [interaction], $p = 0.139$ [drug], and $p = 0.596$ [gene]; $p = 0.008$ [interaction], $p = 0.324$ [drug], and $p = 0.083$ [gene]; for three-week data, $p = 0.985$ [interaction], $p = 0.077$ [drug], and $p = 0.521$ [gene]; $p = 0.575$ [interaction], $p = 0.657$ [drug], and $p < 0.0001$ [gene]; *n* in each bar, number of mice). See also Supplementary Fig. 4 for sniffing time. **J** Sample traces (left) and bar graph (right) of measurements of NMDA/AMPA receptor response ratios recorded from pyramidal neurons in the mPFC of P60-P70 mice one week or three weeks after a single dose D-cycloserine administration (two-way ANOVA, Interaction: $F_{(1, 58)} = 8.930$, $p = 0.004$; 1w vs. 3w: $F_{(1, 58)} = 4.197$, $p = 0.045$; WT vs. KI: $F_{(1, 58)} = 2.228$, $p = 0.141$; *n*, number of neurons recorded from 4 littermates treated with DCS for 1 week and 4 littermates treated with DCS for 3 weeks, respectively). **K** Top: Sample traces of averaged EPSCs recorded 5 minutes before (dark traces) and 25 min after (light traces) LTP induction. Below: Changes in EPSC amplitude induced by 100 Hz stimulation and quantification of EPSCs 25 minutes after stimulation compared to the respective values before stimulation in pyramidal neurons of the KI mice one week or three weeks after a single dose administration of D-cycloserine (Two-tailed unpaired t test, $t = 2.729$, df = 12, $p = 0.018$; *n* in each bar, number of neurons recorded from 5 mice per group).All data were mean ± SEM. $^*p < 0.05$, $^{**}p < 0.01$, $^{***}p < 0.001$.

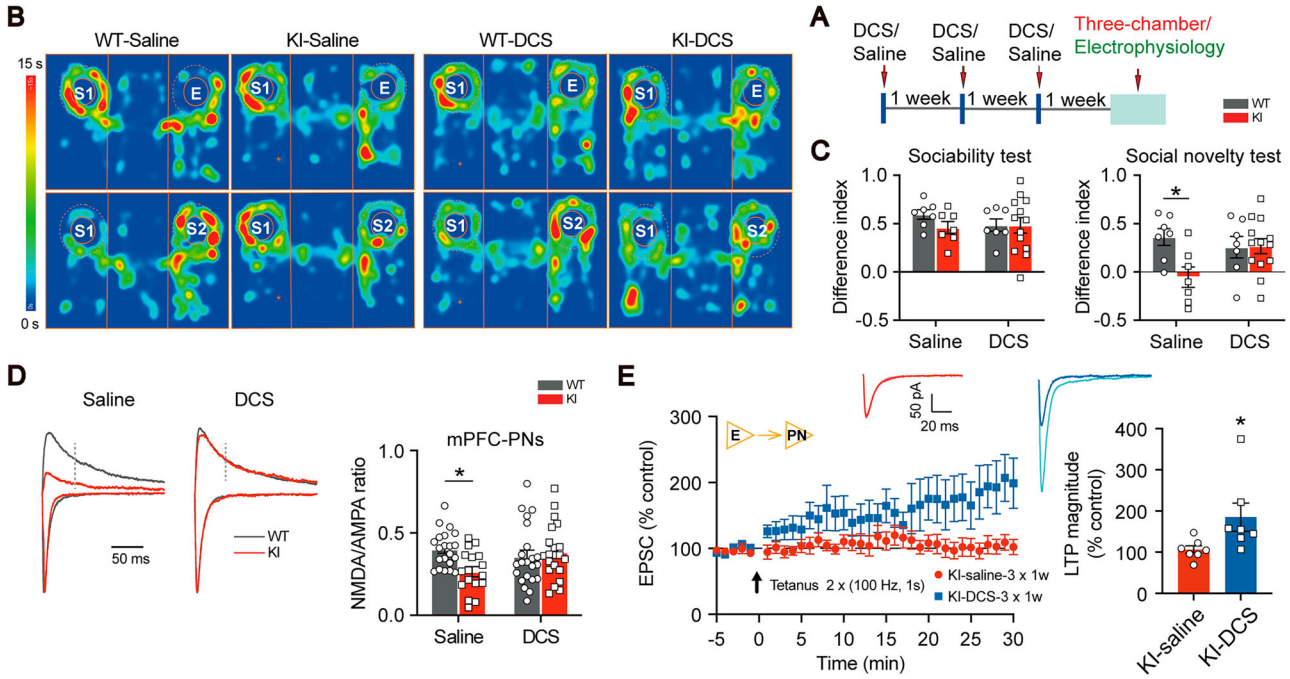


**Fig. 7 | Weekly administration of D-cycloserine is optimal for rescuing social behavioral deficits in the KI mice. A** The flow chart of three-chamber/ electrophysiological tests for examining the rescue effect of DCS administration once a week for three consecutive weeks. **B** Representative heatmaps of the three-chamber tests performed in WT/KI mice one week after three consecutive weeks of saline/ DCS administration. **C** DCS rescued social novelty deficits in the KI mice, as analyzed by the sociability difference index and the social novelty difference index, one week after three consecutive weeks of administration (two-way ANOVA, $p = 0.400$ [interaction], $p = 0.575$ [drug], and $p = 0.382$ [gene]; $p = 0.037$ [interaction], $p = 0.275$ [drug], and $p = 0.047$ [gene]; n in each bar, number of mice). See also Supplementary Fig. 5 for sniffing time. **D** Sample traces (left) and bar graph (right) of measurements of NMDA/AMPA receptor response ratios recorded from pyramidal neurons in the mPFC of P60-P70 mice one week after three consecutive weeks of DCS administration (two-way ANOVA, Interaction: $F_{(1, 77)} = 5.693$, $p = 0.020$; Drug: $F_{(1, 77)} = 1.172$, $p = 0.282$; WT vs. KI: $F_{(1, 77)} = 2.553$, $p = 0.114$; $n$, number of neurons recorded from 4 saline-treated littermates and 4 DCS-treated littermates, respectively). **E** Top: Sample traces of averaged EPSCs recorded 5 min before (dark traces) and 25 min after (light traces) LTP induction. Below: Changes in EPSC amplitude induced by 100 Hz stimulation and quantification of EPSCs 25 min after stimulation compared to the respective values before stimulation in pyramidal neurons of the KI mice one week after three consecutive week administration of saline or D-cycloserine (Two-tailed Mann-Whitney test, $p = 0.011$; n in each bar, number of neurons recorded from 5 mice per group).All data were mean ± SEM. $^*p < 0.05$.

## Discussion

In summary, our study provides compelling evidence that the mPFC harbors social engram cells, which are activated during social interactions and undergo NMDAR-dependent LTP, leading to enhanced synaptic function that regulates social memory. A single mutation in neuroligin 3 disrupts NMDAR-dependent LTP, thereby preventing the formation of social memory engram cells for specific conspecifics, which culminates in social memory deficits. Remarkably, these deficits can be ameliorated by DCS and the optimal therapeutic regimen is a "pulsed" once-weekly administration. These findings highlight the crucial role of NMDAR-dependent LTP in social memory formation during social exploration and underscore the therapeutic potential of targeted pharmacological interventions for alleviating ASD-related social impairments.

Utilizing activity-dependent cell labeling and functional manipulation techniques, we identified a distinct neuronal population encoding social memory information. In contrast to other forms of episodic memory, social memory in rodents is typically detectable only within hours of memory formation through behavioral assays[3,32]. To facilitate the formation of long-term social memories, such as those lasting a week, we exposed the mice to repeated social interactions on five consecutive days, thereby reinforcing the learning process. Notably, this social memory remained retrievable one week later through natural cues. Functional manipulation further confirmed the necessity and sufficiency of these identified neurons for the retrieval of social memory. Comparison of experimental conditions revealed that, regardless of whether the mice remembered the previously encountered conspecifics one week later, the proportion of re-activated neurons involved in social exploration remained unchanged, showing no significant differences. This may reflect the limitations of c-FOS staining, which allows for the quantification of activated neurons during social exploration but does not reveal the precise patterns of neuronal activity during the social process. It is plausible that when social memory can be retrieved and social novelty behaviors are exhibited, the re-activated SMECs may display significantly enhanced activity patterns due to structural and biological alterations within these cells.

Additionally, we observed robust functional plasticity and LTP occlusion in the tagged neurons, further reinforcing the existence of social memory engrams within the mPFC. While social engram cells have been identified in various brain regions, including the mPFC[12], hippocampus[33], and thalamic reticular nucleus[34], the intracellular signaling pathways mediating the plastic changes of these engram cells remain elusive. Our previous work demonstrated that NL3 R451C KI mice exhibit deficits in social novelty preference[9]. Since the social novelty test does not incorporate a defined learning phase or delay period, we performed a more specific assay for social memory—the long-term social memory test—and found that KI mice exhibited impaired social memory. The R451C mutation in Neuroligin 3, a postsynaptic cell adhesion molecule at both excitatory and inhibitory synapses, leads to NMDAR hypofunction[8]. Consequently, the KI mice fail to induce NMDAR-dependent LTP in neurons associated with social stimuli, thereby impeding the maturation of these cells into bona fide SMECs for specific conspecifics. Accordingly, within the KI context, it is more precise to refer to the RAM-labeled neurons as "social exploration-associated neurons" rather than fully established SMECs. In our study, we assessed global NMDAR-dependent LTP in mPFC pyramidal neurons and $PV^+$ interneurons, without selectively isolating social exploration–associated subsets

during electrophysiological recordings. Thus, the plasticity deficits we observed reflect a broad impairment spanning these neuronal classes in KI mice. We posit that the LTP deficits in these neurons arise not from LTP occlusion (as observed in WT SMECs) but rather from a fundamental disruption of NMDAR-dependent plasticity mechanisms. Notably, even the unlabeled neuronal populations in KI mice exhibited comparable impairments in LTP. Strikingly, administration of the NMDAR partial agonist DCS restored neuroplasticity, rescuing the social memory deficits observed in KI mice. Given that neuroplasticity underpins higher-order cognitive processes such as learning and memory[20,35], these findings position DCS as a promising therapeutic candidate for ameliorating memory and learning impairments, particularly in the context of interventions predicated on experience-dependent plasticity.

In addition to pyramidal neurons, our findings reveal that NMDAR-dependent LTP is likewise attenuated in $PV^+$ interneurons. Notably, treatment with 60 μM D-cycloserine exhibited a marked trend toward restoring LTP in these interneurons, although statistical significance was not yet achieved—possibly due to the need for higher concentrations or prolonged pre-incubation. This raises the intriguing possibility that recovery of synaptic plasticity within $PV^+$ interneurons contributes to the behavioral rescue observed following DCS treatment. $PV^+$ interneurons play a central role in governing network oscillations and mediating feed-forward inhibition, both of which are indispensable for ensuring the temporal precision of cortical activity and for regulating information flow within prefrontal circuits[36,37]. Restoration of PV-LTP may therefore enhance the functional integration of inhibitory control, fostering more coherent oscillatory dynamics and stabilizing excitation-inhibition balance during task execution. These network-level refinements may act synergistically with the reinstatement of pyramidal LTP to normalize circuit output, thereby facilitating the observed behavioral recovery. Future studies employing cell-type-specific manipulations will be essential to disentangle the relative contributions of excitatory and inhibitory plasticity to the therapeutic efficacy of DCS.

The NMDAR has emerged as a promising therapeutic target for certain forms of ASDs and schizophrenia[38,39]. The NMDAR partial agonist DCS has been shown to improve sociability in various mouse models of ASDs, as well as in children with ASDs[8,40–43]. However, as previously noted, DCS does not consistently yield positive effects in either ASD patients or animal models[44,45]. This inconsistency may be attributed to the small sample sizes in clinical trials. Additionally, differences in outcomes may arise from whether NMDAR hypofunction is present in ASD patients or mice at the time of DCS administration. Animal models of ASDs exhibit bidirectional NMDAR dysfunction, and correcting this deficit can ameliorate ASD-like behaviors, suggesting that either direction of deviation in NMDAR function contributes to ASD pathophysiology[24]. Therefore, in the treatment of ASD patients, it is essential to select appropriate interventions based on the specific alterations in NMDAR function, emphasizing the importance of precision medicine.

A partial agonist, such as DCS, is less likely to induce undesirable excitotoxic effects or desensitization of the glycine-binding site, especially with chronic administration, compared to full agonists. Thus, exploring the longest effective dosing period of DCS without reducing receptor sensitivity or causing other side effects is crucial. In a double-blind randomized trial with 20 older adolescents and young adults with ASDs, two DCS dosing strategies (50 mg daily vs. 50 mg weekly) were tested over 8 weeks, with a 2-week follow-up after discontinuation. Statistically and clinically significant improvements were observed on the Social Responsiveness Scale and the Aberrant Behavior Checklist, particularly in the subscales of "lethargy/social withdrawal" and "stereotypic behavior"[46,47]. However, the specific mechanisms underlying the differential efficacy of these dosing strategies remain unclear. The half-life of DCS varies between 8 and 12 h, depending on renal function[48]. Our results suggest that a single dose of DCS can effectively rescue NMDAR function and NMDAR-dependent LTP in the KI mice for at least one week, supporting the notion that "pulsed" once-weekly administration is both optimal and well-tolerated, although the precise molecular mechanisms warrant further investigation.

## Methods

### Animals

To facilitate electrophysiological recordings of $PV^+$ interneurons, CB6-Tg(Gad1-EGFP)G42Zjh/J (G42; Jackson Laboratory strain 007677) mice were crossed with B6;129-Nlgn3$^{tm1Sud}$/J (Neuroligin-3 R451C knock-in; Jackson Laboratory strain 008475) mice, both maintained on a C57BL/6 J background. Because the *Nlgn3* gene resides on the X chromosome, experimental cohorts were generated by crossing heterozygous mutant females with WT males, thereby producing both WT and KI male offspring for downstream analyses. In some experiments, only WT (C57BL/6 J) mice purchased from Shanghai SLAC Laboratory were used. Animals were randomly assigned to experimental groups. For some experiments, recordings were randomly collected from littermate mice. All mice were maintained under a 12 h light/dark cycle at 22–25 °C, with ad libitum access to tap water and standard chow. Four or five mice were housed per cage. Young adult male mice (2–3 months old) were used in all experiments. We have complied with all relevant ethical regulations for animal use. All experimental procedures were approved by the Laboratory Animal Welfare and Ethics Committee of Hangzhou Normal University, and by the Institutional Animal Care and Use Committee of Zhejiang University.

### Slice preparation

Mice were deeply anesthetized with sodium pentobarbital (75 mg/kg, i.p.) and decapitated. The brain was quickly removed and placed in ice-cold, high-sucrose artificial cerebrospinal fluid (ACSF) containing (in mM): 194 sucrose, 30 NaCl, 4.5 KCl, 1.2 $NaH_2PO_4$, 26 $NaHCO_3$, 10 glucose, 0.2 $CaCl_2$, and 2 $MgCl_2$, oxygenated with 95% $O_2$ and 5% $CO_2$. Coronal slices (300 μm thick) containing PFC were cut on a vibratome (Leica VT1200S). The slices were stored in a submerged holding chamber for 25–35 min at 34 °C in oxygenated ACSF to maintain a pH of approximately 7.4, and were then kept at room temperature until use. The ACSF consisted of (in mM): 119 NaCl, 2.5 KCl, 11 glucose, 1.0 $NaH_2PO_4$, 26.2 $NaHCO_3$, 2.5 $CaCl_2$, and 1.3 $MgCl_2$.

### Electrophysiology

Whole-cell recordings were performed in the medial prefrontal cortex, encompassing the anterior cingulate, prelimbic, and infralimbic regions. Individual slices were transferred to a recording chamber and continuously perfused with ACSF (2 ml/min) oxygenated with 95% $O_2$ and 5% $CO_2$ and maintained at 34 ± 2 °C. EGFP-expressing $PV^+$ basket interneurons were identified based on two criteria: a round/oval shape and soma diameter >10 μm, and the presence of multipolar dendritic trees lacking apparent apical and/or basal dendrites. The series resistance ($R_a$) was 10–20 MΩ and monitored on-line throughout experiments; the data were discarded when the $R_a$ changement was over 20%.

For NMDA/AMPA experiments in layer V/VI neurons, a concentric bipolar electrode was placed in layer II/III. The recording pipettes (3–5 MΩ) were filled with an internal solution containing (in mM): 115 $CsMeSO_4$, 20 CsCl, 10 HEPES, 2.5 $MgCl_2$, 4 Na-ATP, 0.4 $Na_2$-GTP, 10 NaPhosphocreatine, 0.6 EGTA and 5 QX-314 (pH 7.2; 290-310 mOsm). Picrotoxin (100 μM; MCE, China, HY-101391) was included throughout to block $GABA_A$ receptor-mediated currents. Pyramidal neurons were voltage-clamped at −70 mV, and excitatory postsynaptic currents (EPSCs) were evoked at 0.1 Hz. AMPA receptor-mediated EPSCs were recorded at −70 mV, and 30 consecutive responses were recorded after stable baseline. After recording AMPA receptor-mediated EPSCs, holding potential was changed to +40 mV to record NMDAR-mediated EPSCs. 30 consecutive traces were averaged to obtain mean current trace of AMPA and NMDAR-mediated EPSCs. NMDAR-mediated EPSC currents were measured 50 ms after stimulus.

For paired-pulse ratio (PPR) recordings, cells were held at −70 mV. Picrotoxin (100 μM; MCE, China, HY-101391) was consistently applied to block $GABA_A$ receptor-mediated currents. PPR was calculated as the ratio of the amplitude of the second eEPSC to that of the first. To calculate the mean PPR, we recorded 15–30 individual traces, calculated the PPR for each trace, and averaged the results. The intervals of the first and second eEPSC were 30, 50, 100, 150 and 200 ms. For AMPA receptor-mediated EPSC input-output recordings, cells were recorded at −70 mV. We recorded 15–30 consecutive responses at varying stimulus intensities and averaged them separately.

For whole-cell LTP recordings, AMPA receptor-mediated EPSCs were recorded at −70 mV. Picrotoxin (100 μM; MCE, China, HY-101391) was consistently present to block $GABA_A$ receptor-mediated currents. After recording a stable baseline for 5 min, a single high-frequency stimulus (HFS; 100 Hz for 1 s) was continuously used twice to induce LTP while cells were depolarized to 0 mV. In some cases, LTP was induced by three trains of theta-burst stimulation (each train consisting of four bursts of 5 pulses at 100 Hz delivered at 200 ms intervals) separated by 30 s, paired with four 60 ms depolarization steps to −10 mV. These induction protocols were applied within 10 min to achieve the whole-cell configuration and avoid the "wash-out" of LTP. Recording was continued for a further 30 min to monitor the LTP process. The LTP magnitude was determined by the averaged eEPSC amplitudes during the 25–30 min after LTP induction compared with those during the 2–5 min baseline. In some experiments, 50 μM D-AP5 (MCE, China, HY-100714A) were added to the bath solution to block NMDARs and prevent LTP induction.

For whole-cell LTD recordings, recording pipettes were filled with solution containing (in mM): 145 K-gluconate, 5 NaCl, 1 $MgCl_2$, 0.2 EGTA, 10 HEPES, 2 Mg-ATP and 0.1 $Na_3$-GTP (pH 7.2; 290-310 mOsm). After obtaining stable EPSCs for at least 5 min, LTD was induced by 300 pulses at 1 Hz paired with postsynaptic depolarization at −45 mV.

All recordings were made with an Axon 700B amplifier and 1550B digitizer (Molecular Devices, Sunnyvale, CA, USA). Responses were filtered at 3 kHz, digitized at 10 kHz and analyzed using Clampfit 10.4 (Molecular Devices).

### Immunohistochemistry

Animals were deeply anesthetized with an overdose of sodium pentobarbital (≥100 mg/kg, i.p.) and then transcardially perfused with saline, followed by 4% paraformaldehyde in phosphate buffered saline (PBS, 0.01 M, pH 7.4, 4 °C). Intact brains were extracted and post-fixed in 4% paraformaldehyde (Sigma, 441244) overnight at 4 °C, and then cryoprotected in 25% sucrose (Solarbio, S8271) solution (pH 7.4) for 48 h. The tissue was coronal sectioned at 30 μm on a sliding freezing microtome (Thermo Scientific CryoStar NX50). For c-Fos staining, sections were blocked in PBS containing 5% bovine serum albumin (BSA; Sigma, V900933) and 0.7% Triton X-100 (Solarbio, T8200) overnight at 4 °C, and then incubated in a mixture of primary antibody in PBS containing 5% BSA and 0.7% Triton X-100 in room temperature for 4 h. For CamKII and GAD67 staining, sections were blocked in PBS containing 5% BSA and 0.3% Triton X-100 overnight at 4 °C, and then incubated in a mixture of primary antibody in PBS containing 5% BSA and 0.3% Triton X-100 for 2 days at 4 °C. After 3 times of rinses in PBS per 10 min, tissues were incubated with secondary antibody in PBS for 2 h, washed with PBS for 3 times, mounted using Mowiol mounting medium (Sigma, 81381), and imaged under a fluorescence microscope.

### Microscopy, image processing and analysis

Slides were visualized under the OLYMPUS VS200 microscope. Images were captured with the same parameters and were analyzed blindly. Brain regions were defined by the Mouse Brain in Stereotaxic Coordinates (interaural 5.58 mm, bregma 1.78 mm for the mPFC). Signals were counted from 2–5 slices per mouse at the labeled Bergman position. The control and experimental groups were processed in parallel and samples from at least 3 groups of mice were analyzed.

### Antibodies

The following antibodies were using: c-Fos (1:800; rabbit, ABclonal, A24620), CamKII (1:50; goat, Invitrogen, PA5-19128), GAD67 (1:400; mouse, Sigma, MAB5406). Secondary antibodies were purchased from Invitrogen (Goat anti-Rabbit DyLight-550, 1:1000, 84541; Donkey anti-Goat Alexa Fluor-647, 1:1000, A-21447; Goat anti-Mouse Alexa Fluor-594, 1:1000, A-11005).

### Microinjection

For induction, mice were rapidly anesthetized with isoflurane (5%; RWD, China, R510-22-10) in an induction chamber. They were then maintained under deep anesthesia with isoflurane (1-2%, as needed) and secured in a stereotaxic frame. Local analgesia was provided by subcutaneous infiltration of bupivacaine (0.25%, <20 μL; MCE, China, HY-B0405) along the incision line. An incision was made in the skin over the skull to expose the bregma, lambda, and the target injection site. The stereotactic coordinates relative to bregma (AP + 1.90 mm, LM ± 0.40 mm, DV −2.3 mm) were used for AAV injections. Two small drill holes were made in the skull over the injection site to expose the brain. The AAVs used in this study were diluted to ~$10^{12}$ vector genomes (v.g.)/mL and purchased from BrainVTA Ltd., Wuhan.

For RAM labeling, AAV2/9-RAM-d2TTA:TRE-EGFP (PT-0627) was bilaterally injected (500 nL per hemisphere). For CRAM activation experiments, AAV2/9-RAM-d2TTA:TRE-Cre-EGFP (PT-2625) and rAAV-hSyn-DIO-hM3D(Gq)-mCherry (PT-0019) were bilaterally injected (600 nL per hemisphere). For CRAM inhibition experiments, AAV2/9-RAM-d2TTA:-TRE-Cre-EGFP (PT-2625) and AAV2/9-hSyn-DIO-hM4D(Gi)-mCherry (PT-0020) were bilaterally injected (600 nL per hemisphere).

### Behavioral tests

All behavioral assays were performed with age-matched male mice littermates (8–12 weeks). All behavior studies were performed during day times (light-on periods). Mice were handled daily for at least 3 min per day for 7 days until mice were habituated to the operator.

### Three-chamber social interaction assay

Three-chambered apparatus was 60 × 40 × 25 cm with a 20 cm-wide center chamber and 20 cm-wide side chambers. In the first phase, a subject mouse was placed in the apparatus and was allowed to explore the environment freely for 10 min for habituation. After 10 min, the mouse was gently guided to the center chamber, and the two entrances to the center chamber were blocked while a stranger C57BL/6 J mouse (Stranger 1) was placed in one container. The position of stranger 1 was alternated between tests to prevent side preference of the object mouse. The two entrances were then opened to allow the subject mouse to explore the new environment freely for 10 min. In the third phase, stranger 2 was placed in the other empty container and the subject mouse again freely explored all three chambers for 10 min. All stranger mice were males at the same age and previously habituated to the plastic cage during the previous day for 30 min. The box was wiped with 75% ethanol and air-dried between mice. The videos were recorded by a video camera, and the sniffing time was calculated manually and blindly by others. Sniffing time was defined as each instance in which a mouse's nose touched the container or was oriented toward the container and came within 4 cm of distance. In addition to sniffing time, we also calculated the deference index, which represents a numerical difference between times spent exploring the targets (Stranger1 vs. Empty, or Stranger 2 vs. Stranger 1) divided by total time spent exploring both targets.

### Long-term social memory assay

A 40 × 40 × 40 cm open field box was used for this task. During the habituation phase (days 1–5), a subject mouse was placed in the box with a stranger C57BL/6 J mouse (Stranger 1, S1) contained in a small container. The animals were allowed to freely explore the cage and interact with Stranger 1 for 10 min. At the end of each trial, the experimental and stimulus mice were returned to their home cages. For five consecutive days, the experimental

mouse was exposed to the same conspecific (S1) and habituated to the environment and the social stimulus. After one week, the subject mouse was placed in the box with Stranger 1 again to test long-term social memory. Day 12 consisted of the novelty phase, during which a nonfamiliar conspecific (Stranger 2, S2) was placed in the cage with the experimental mouse for 10 min to allow social interaction. In total, the experimental mice were exposed to two different conspecifics: one social stimulus repeatedly presented from days 1–5 (habituation phase, S1) and day 11 (long-term social memory test phase, S1), as well as a second mouse on day 12 (novelty phase, S2). The box was wiped with 75% ethanol and air-dried between mice. Sniffing time was defined as each instance in which a mouse's nose touched the container, or was oriented toward the container and came within 4 cm of it.

### Engram labeling

For RAM or CRAM labeling, mice were maintained on doxycycline (Dox, 60 mg/L; Selleck, S4163) in their drinking water following AAV injections. Animals were transitioned to Dox-free water 24 h before and after the labeling phase. To selectively manipulate social memory-tagged neurons, DCZ (50 μg/kg, i.p.; MCE, China, HY-42110) was administered 90 min prior to behavioral assessments.

Before labeling, mice were singly housed for one week. To label social memory engram cells, mice were introduced to a novel stimulus (C57BL/6 J, 6-7 weeks old male mice; Stranger 1) within their home cages, minimizing neuronal labeling due to environmental noise. A researcher closely monitored interactions, and any mice exhibiting aggressive behavior were excluded from further experimentation. To visualize social memory engrams, subject mice were allowed to interact with the social stimulus for 10 min. After this interaction period, the subject and stimulus mice were separated for one week. For immunofluorescence staining of engram cells, mice were re-exposed to either the familiar stimulus (Stranger 1) or a novel stimulus (Stranger 2) for 10 min, 90 min before sacrifice. For chemogenetic activation of engram cells, subject mice were allowed a one-hour interaction with the social stimulus for labeling.

An alternative labeling method was employed in conjunction with a long-term social memory assay. Prior to labeling, mice were individually housed for one week. During this period, the mice were exposed to a confined C57BL/6 J mouse (Stranger 1, S1) within a small enclosure placed in the open-field arena or in homecages containing freely moving novel mice, across five distinct sessions. Social memory engram cells were labeled during the fifth exposure. After this interaction, the subject and stimulus mice were separated for one week. For immunofluorescence staining of engram cells, mice were re-exposed to either the familiar stimulus mouse (S1) or a novel stimulus (Stranger 2, S2) for 10 min, 90 min before sacrifice. For chemogenetic inhibition of engram cells, subject mice were allowed a one-hour interaction with the social stimulus for labeling.

### Drug application

In the LTP recording experiments, D-cycloserine (MCE, China, HY-B0030; 20 μM for pyramidal neurons and 60 μM for $PV^+$ interneurons) was bath-applied for 20 min prior to and throughout the entire recording session.

WT and KI mice received intraperitoneal injections of D-cycloserine (20 mg/kg) or an equivalent volume of saline either one week or three weeks before the three-chamber assays. In a separate set of behavioral experiments, WT and KI mice were administered intraperitoneal injections of D-cycloserine (20 mg/kg) or an equivalent volume of saline once weekly for three consecutive weeks, beginning one week prior to the three-chamber assays.

### Statistics and reproducibility

Before starting experiments, based on our previous behavioral studies, we estimated the sample size by using G*Power software. For each experimental cohort undergoing immunohistochemical and electrophysiological analyses, data were obtained from a minimum of three biological replicates (individual mice), ensuring the robustness and reproducibility of the findings. An evaluator blinded to the group assignments performed the assessment and analyzed the data. Only animals with correct virus injection were included in the analysis; no further animals or data points were excluded. Offline analysis of whole-cell patch-clamp data was performed using Clampfit 10.4. Statistical analyses were conducted using Graphpad Prism 10. Unless otherwise specified, comparisons between two groups were made using an unpaired, two-tailed Student's *t*-test. Multiple comparisons were performed using either a one-way ANOVA or a two-way ANOVA. All data are presented as the mean ± SEM. In all cases, $p < 0.05$ was considered statistically significant. $^*p < 0.05$, $^{**}p < 0.01$, $^{***}p < 0.001$. Data sets are available at Mendeley Data[49].

### Reporting summary

Further information on research design is available in the Nature Portfolio Reporting Summary linked to this article.

## Data availability

Numerical source data for all figures are provided in Supplementary Data 1 and in the dataset by Cao, Wei; Li, Zhiyuan (2025), "Social Memory Engram Formation Impairment in Neuroligin-3 R451C Knock-in Mice is Caused by Disrupted Prefrontal NMDA Receptor-Dependent Potentiation", Mendeley Data, V1, doi: 10.17632/v2twstbh3c.1. Correspondence and requests for materials should be addressed to Wei Cao or Baoming Li.

Received: 13 February 2025; Accepted: 27 August 2025;
Published online: 30 September 2025

## References

1. Lyall, K. et al. The Changing Epidemiology of Autism Spectrum Disorders. *Annu Rev. Pub. Health* **38**, 81–102 (2017).
2. Okuyama, T. et al. A neural mechanism underlying mating preferences for familiar individuals in medaka fish. *Science* **343**, 91–94 (2014).
3. Okuyama, T., Kitamura, T., Roy, D. S., Itohara, S. & Tonegawa, S. Ventral CA1 neurons store social memory. *Science* **353**, 1536–1541 (2016).
4. Green, M. F., Horan, W. P. & Lee, J. Social cognition in schizophrenia. *Nat. Rev. Neurosci.* **16**, 620–631 (2015).
5. Bicks, L. K., Koike, H., Akbarian, S. & Morishita, H. Prefrontal Cortex and Social Cognition in Mouse and Man. *Front Psychol.* **6**, 1805 (2015).
6. Barak, B. & Feng, G. Neurobiology of social behavior abnormalities in autism and Williams syndrome. *Nat. Neurosci.* **19**, 647–655 (2016).
7. Mack, N. R., Bouras, N. N. & Gao, W. J. Prefrontal regulation of social behavior and related deficits: insights from rodent studies. *Biol. Psychiatry*, https://doi.org/10.1016/j.biopsych.2024.03.008 (2024).
8. Cao, W. et al. NMDA receptor hypofunction underlies deficits in parvalbumin interneurons and social behavior in neuroligin 3 R451C knockin mice. *Cell Rep.* **41**, 111771 (2022).
9. Cao, W. et al. Gamma Oscillation Dysfunction in mPFC Leads to Social Deficits in Neuroligin 3 R451C Knockin Mice. *Neuron* **97**, 1253–1260.e1257 (2018).
10. Cao, W., Li, H. & Luo, J. Prefrontal cortical circuits in social behaviors: an overview. *J. Zhejiang Univ. Sci. B* **25**, 941–955 (2024).
11. Ma, X. et al. eEF2 in the prefrontal cortex promotes excitatory synaptic transmission and social novelty behavior. *EMBO Rep.* **23**, e54543 (2022).
12. Xing, B. et al. A Subpopulation of Prefrontal Cortical Neurons Is Required for Social Memory. *Biol. Psychiatry* **89**, 521–531 (2021).
13. de Leon Reyes, N. S. et al. Corticotropin-releasing hormone signaling from prefrontal cortex to lateral septum suppresses interaction with familiar mice. *Cell* **186**, 4152–4171.e4131 (2023).
14. DeNardo, L. & Luo, L. Genetic strategies to access activated neurons. *Curr. Opin. Neurobiol.* **45**, 121–129 (2017).
15. Kitamura, T. et al. Engrams and circuits crucial for systems consolidation of a memory. *Science* **356**, 73–78 (2017).
16. DeNardo, L. A. et al. Temporal evolution of cortical ensembles promoting remote memory retrieval. *Nat. Neurosci.* **22**, 460–469 (2019).
17. Hua, S. S. et al. NMDA Receptor-Dependent Synaptic Potentiation via APPL1 Signaling Is Required for the Accessibility of a Prefrontal

Neuronal Assembly in Retrieving Fear Extinction. *Biol. Psychiatry* **94**, 262–277 (2023).
18. Tonegawa, S., Liu, X., Ramirez, S. & Redondo, R. Memory Engram Cells Have Come of Age. *Neuron* **87**, 918–931 (2015).
19. Lisman, J., Yasuda, R. & Raghavachari, S. Mechanisms of CaMKII action in long-term potentiation. *Nat. Rev. Neurosci.* **13**, 169–182 (2012).
20. Whitlock, J. R., Heynen, A. J., Shuler, M. G. & Bear, M. F. Learning induces long-term potentiation in the hippocampus. *Science* **313**, 1093–1097 (2006).
21. Nicoll, R. A. A Brief History of Long-Term Potentiation. *Neuron* **93**, 281–290 (2017).
22. Zoodsma, J. D. et al. Disruption of grin2B, an ASD-associated gene, produces social deficits in zebrafish. *Mol. Autism* **13**, 38 (2022).
23. O'Roak, B. J. et al. Multiplex targeted sequencing identifies recurrently mutated genes in autism spectrum disorders. *Science* **338**, 1619–1622 (2012).
24. Lee, E. J., Choi, S. Y. & Kim, E. NMDA receptor dysfunction in autism spectrum disorders. *Curr. Opin. Pharm.* **20**, 8–13 (2015).
25. Lee, K., Mills, Z., Cheung, P., Cheyne, J. E. & Montgomery, J. M. The Role of Zinc and NMDA Receptors in Autism Spectrum Disorders. *Pharmaceuticals (Basel)* **16**, https://doi.org/10.3390/ph16010001 (2022).
26. Sorensen, A. T. et al. A robust activity marking system for exploring active neuronal ensembles. *Elife* **5**, https://doi.org/10.7554/eLife.13918 (2016).
27. Zheng, Z. et al. A small population of stress-responsive neurons in the hypothalamus-habenula circuit mediates development of depression-like behavior in mice. *Neuron* **112**, 3924–3939.e3925 (2024).
28. Zheng, Z. et al. Hypothalamus-habenula potentiation encodes chronic stress experience and drives depression onset. *Neuron* **110**, 1400–1415.e1406 (2022).
29. Ehrlich, I. & Malinow, R. Postsynaptic density 95 controls AMPA receptor incorporation during long-term potentiation and experience-driven synaptic plasticity. *J. Neurosci.* **24**, 916–927 (2004).
30. Goff, D. C. et al. Once-weekly D-cycloserine effects on negative symptoms and cognition in schizophrenia: an exploratory study. *Schizophr. Res* **106**, 320–327 (2008).
31. Quartermain, D., Mower, J., Rafferty, M. F., Herting, R. L. & Lanthorn, T. H. Acute but not chronic activation of the NMDA-coupled glycine receptor with D-cycloserine facilitates learning and retention. *Eur. J. Pharm.* **257**, 7–12 (1994).
32. Bluthe, R. M., Gheusi, G. & Dantzer, R. Gonadal steroids influence the involvement of arginine vasopressin in social recognition in mice. *Psychoneuroendocrinology* **18**, 323–335 (1993).
33. Watarai, A., Tao, K., Wang, M. Y. & Okuyama, T. Distinct functions of ventral CA1 and dorsal CA2 in social memory. *Curr. Opin. Neurobiol.* **68**, 29–35 (2021).
34. Wang, F. et al. The thalamic reticular nucleus orchestrates social memory. *Neuron* **112**, 2368–2385.e2311 (2024).
35. Gruart, A., Munoz, M. D. & Delgado-Garcia, J. M. Involvement of the CA3-CA1 synapse in the acquisition of associative learning in behaving mice. *J. Neurosci.* **26**, 1077–1087 (2006).
36. Faini, G. et al. Perineuronal nets control visual input via thalamic recruitment of cortical PV interneurons. *Elife* **7**, https://doi.org/10.7554/eLife.41520 (2018).
37. Contractor, A., Ethell, I. M. & Portera-Cailliau, C. Cortical interneurons in autism. *Nat. Neurosci.* **24**, 1648–1659 (2021).
38. Deutsch, S. I. & Burket, J. A. From Mouse to Man: N-Methyl-d-Aspartic Acid Receptor Activation as a Promising Pharmacotherapeutic Strategy for Autism Spectrum Disorders. *Med Clin. North Am.* **107**, 101–117 (2023).
39. Kruse, A. O. & Bustillo, J. R. Glutamatergic dysfunction in Schizophrenia. *Transl. Psychiatry* **12**, 500 (2022).
40. Won, H. et al. Autistic-like social behaviour in Shank2-mutant mice improved by restoring NMDA receptor function. *Nature* **486**, 261–265 (2012).
41. Wu, H. F. et al. D)-Cycloserine Ameliorates Autism-Like Deficits by Removing GluA2-Containing AMPA Receptors in a Valproic Acid-Induced Rat Model. *Mol. Neurobiol.* **55**, 4811–4824 (2018).
42. Posey, D. J. et al. A pilot study of D-cycloserine in subjects with autistic disorder. *Am. J. Psychiatry* **161**, 2115–2117 (2004).
43. Wink, L. K. et al. d-Cycloserine enhances durability of social skills training in autism spectrum disorder. *Mol. Autism* **8**, 2 (2017).
44. Minshawi, N. F. et al. A randomized, placebo-controlled trial of D-cycloserine for the enhancement of social skills training in autism spectrum disorders. *Mol. Autism* **7**, 2 (2016).
45. Chung, C. et al. Early Correction of N-Methyl-D-Aspartate Receptor Function Improves Autistic-like Social Behaviors in Adult Shank2(-/-) Mice. *Biol. Psychiatry* **85**, 534–543 (2019).
46. Urbano, M. et al. A trial of D-cycloserine to treat stereotypies in older adolescents and young adults with autism spectrum disorder. *Clin. Neuropharmacol.* **37**, 69–72 (2014).
47. Urbano, M., Okwara, L., Manser, P., Hartmann, K. & Deutsch, S. I. A trial of d-cycloserine to treat the social deficit in older adolescents and young adults with autism spectrum disorders. *J. Neuropsychiatry Clin. Neurosci.* **27**, 133–138 (2015).
48. Peloquin, C. A. *Clinical pharmacology of the antituberculosis drugs*. Fourth Edition edn, Vol. Clinical tuberculosis 205–224 (CRC Press, 2008).
49. Cao, W. & Li, Z. Y. Social Memory Engram Formation Impairment in Neuroligin-3 R451C Knock-in Mice is Caused by Disrupted Prefrontal NMDA Receptor-Dependent Potentiation [Data set]. https://doi.org/10.17632/v2twstbh3c.1 (2025).

## Acknowledgements

This work was supported by grants from the National Natural Science Foundation of China (81801355 and 32471067 to W.C., and U22A20306 to J.-h. Luo), the Autism Research Special Fund of Zhejiang Foundation For Disabled Persons (2023002 to W.C.), and the Ministry of Science and Technology of China (STI 2030-Major Project 2021ZD0201705 to B.L.).

## Author contributions

W.C. and B.L. conceived and designed the experiments. Z.L. and H.Y. conducted the electrophysiological recordings. Q.Y. and J.-h. Li carried out the behavioral experiments. H.L. and J.G. performed the immunohistochemical analyses. Y.F., K.Y., S.L., J.C., and W.D. were responsible for animal care and genotyping. W.C., B.L., J.-h. Luo, and J.X. wrote the manuscript. All authors reviewed and provided comments on the manuscript.

## Competing interests

The authors declare no competing interests.

## Additional information

**Supplementary information** The online version contains supplementary material available at https://doi.org/10.1038/s42003-025-08806-1.

**Correspondence** and requests for materials should be addressed to Baoming Li or Wei Cao.

**Peer review information** *Communications Biology* thanks Luye Qin and the other, anonymous, reviewer(s) for their contribution to the peer review of this work. Primary Handling Editors: Christoph Anacker and Rosie Bunton-Stasyshyn. A peer review file is available.